Research Square

Preprints are preliminary reports that have not undergone peer review.
They should not be considered conclusive, used to inform clinical practice,
or referenced by the media as validated information.

APLP2 as a Molecular Link Between Immune Regulation and Bone Metabolism in Hepatocellular Carcinoma: Evidence from scRNA-Seq and Functional Validation

Zhen Liang
Macau University of Science and Technology
Jinchang Zheng
Macau University of Science and Technology
Zhanpeng Su
Affiliated Hospital of Guangdong Medical University
Bo Wu
Affiliated Hospital of Guangdong Medical University
Haina Yang
Affiliated Hospital of Guangdong Medical University
Shuyou Bai
Macau University of Science and Technology
Xinyuan Wu
Affiliated Hospital of Guangdong Medical University
Chong Sun
Affiliated Hospital of Guangdong Medical University
Litao Duan
Zhongshan Institute for Drug Discovery
Shaoru Chen
Zhongshan Institute for Drug Discovery
Bo Wei
Macau University of Science and Technology
Xingxing Fan
Macau University of Science and Technology
Sien Lin
sienlin@hku.hk

Macau University of Science and Technology

Research Article

Keywords: hepatocellular carcinoma, single-cell RNA sequencing, bone metabolism, immunity, heterogeneity

Posted Date: December 11th, 2025

DOI: https://doi.org/10.21203/rs.3.rs-7785516/v1

License: This work is licensed under a Creative Commons Attribution 4.0 International License. Read Full License

Additional Declarations: No competing interests reported.

Version of Record: A version of this preprint was published at Cancer Cell International on June 14th, 2026. See the published version at https://doi.org/10.1186/s12935-026-04365-5.

Abstract

Background and Aims: Hepatocellular carcinoma (HCC) remains a significant health concern worldwide, characterized by elevated mortality rates that are often associated with diagnoses occurring in advanced stages and the restricted efficacy of treatment options currently available. Immune checkpoint inhibitors (ICIs) demonstrate promise in treating HCC; nonetheless, challenges related to therapeutic resistance and varied responses among patients underscore the necessity of identifying new biomarkers and comprehending the fundamental mechanisms involved. This research explores the molecular relationship between immune regulation and bone metabolism in HCC by employing integrated single-cell RNA sequencing (scRNA-seq), bulk transcriptomics, and functional validation.

Methods: The analysis of publicly accessible scRNA-seq (GSE223204) and bulk RNA-seq (TCGA-LIHC) datasets was conducted to discover distinct cell subpopulations and signaling patterns. Clustering, ligand-receptor interaction analysis, and transcription factor mapping were performed using the Seurat, CellChat, and SCENIC pipelines. A random survival forest method helped identify important prognostic genes. The research examined how immune cells infiltrate and their relationship with components that regulate the immune response. Clinical HCC samples were obtained for validation using qPCR. The functional effects of the gene APLP2 were studied through small interfering RNA (siRNA) knockdown experiments in HCC cell lines and co-culturing with osteoblasts.

Results: In the tissues of HCC, nine distinct cell types were recognized, where hepatocytes demonstrated significant involvement in pathways related to bone metabolism and immune functions. Seven key genes (APLP2, SERPINC1, CAT, PDIA6, SLC2A2, C1S, and CFB) were found to be prognostically significant and closely linked to immune cell infiltration, immunomodulatory checkpoints, and key metabolic signaling pathways, including WNT/β-catenin and PI3K-AKT-mTOR. Particularly, APLP2 showed increased expression specifically in cancerous tissues. Reduced APLP2 levels suppressed proliferation, invasion, migration, and promoted apoptosis in HCC cells. Moreover, the downregulation of APLP2 lessened the suppressive influence of tumor cells on osteoblast differentiation, indicating its potential regulatory function in bone metabolism.

Conclusion: This research highlights APLP2 as a new molecular connector between immune evasion and dysregulation of bone metabolism in HCC. The combination of single-cell analysis along with experimental validation offers fresh perspectives on the underlying mechanisms of immunotherapy resistance and emphasizes APLP2 as a promising dual-function therapeutic target.

1. Introduction

Hepatocellular carcinoma holds a leading position in global cancer incidence rankings(1). As indicated by global cancer statistics, HCC is especially widespread in numerous developing nations, with its development closely linked to risk factors like hepatitis virus infections, cirrhosis, obesity, diabetes, and alcohol use. The rates of incidence and mortality associated with HCC have been increasing(2, 3). The main approaches to treating HCC currently involve surgical removal and liver transplantation, but their

use in clinical settings is frequently restricted by several limitations. A limited number of patients with HCC qualify for surgical interventions, and many are diagnosed at more advanced stages, which negatively impacts patient outcomes(4). Therefore, there is a pressing necessity for innovative therapeutic approaches.

Immunotherapy marks a major progress in HCC treatment. ICIs targeting programmed cell death-1 (PD-1) and its corresponding ligand, programmed cell death ligand 1 (PD-L1), operate by obstructing crucial pathways that allow cancer cells to avoid detection by the immune system, thus revitalizing the body's capability to combat tumors. Currently, these agents are considered vital treatment alternatives for advanced HCC(5, 6). Nevertheless, the variability of HCC across different patients results in unpredictable treatment effects, adverse reactions to drugs, and both innate and acquired resistance to therapy(7–10). This variety has led to efforts to identify biomarkers and signaling pathways that might predict responses to immunotherapy and enhance treatment results.

The latest discoveries have established a connection between the development of HCC and the processes of ossification, along with changes in bone marrow constituents(11). Tumor cells engage with a variety of cellular types present in the bone marrow, such as the vascular system, immune cells, adipocytes, and neurons. These interactions play a role in bone metabolism by modifying the functions of osteoclasts and osteoblasts, thus facilitating bone degradation(12, 13). Additionally, the excessive production of fibroblast growth factor 23 induced by tumors results in the loss of phosphate in the kidneys and leads to hypophosphatemia, which subsequently exacerbates osteomalacia(14). Malignant cells are also capable of stimulating osteoclast activity through the release of parathyroid hormone-related protein or various cytokines(14). Bone degradation has been recognized as a factor contributing to a poor prognosis in individuals diagnosed with HCC. Consequently, it is essential to understand the variety, immune landscape, and possible therapeutic targets associated with HCC to improve patient outcomes.

Due to advancements in bioinformatics, particularly in scRNA-seq technology, scientists can now explore the complex mechanisms underlying HCC with significant detail(15, 16). In this research, scRNA-seq was utilized in tandem with transcriptomic data to conduct a thorough examination of HCC heterogeneity. This study emphasizes the penetration of immune cells, the interactions among various cell types, significant genes, and signaling pathways, as well as the co-expression of genes linked to both HCC and bone metabolism, indicating new possible therapeutic approaches.

2. Materials and Methods

2.1 Data Acquisition

These datasets utilized for the single-cell analysis, associated with GSE223204, were sourced from the Gene Expression Omnibus (GEO) repository, accessible at [GEO Datasets] (https://www.ncbi.nlm.nih.gov/geo/info/datasets.html). Two distinct samples were collected, providing

comprehensive single-cell expression profiles: one originating from a disease context and the other functioning as a control. Additionally, the raw mRNA expression data associated with HCC were sourced from The Cancer Genome Atlas (TCGA) database (https://portal.gdc.cancer.gov/), which includes 374 cancer samples and 50 normal samples.

2.2 Single-Cell Data Quality Assessment

The expression profiles were processed using the Seurat package. Cells were filtered according to the total count of unique molecular identifiers (UMIs), the number of expressed genes, and the ratio of mitochondrial expression for each individual cell. Quality control procedures were carried out using the median absolute deviation (MAD) approach. A data point was deemed an outlier if it was more than three MADs from the median and was subsequently excluded from further analysis. Subsequently, the DoubletFinder tool (V2.0.4) was utilized to detect and eliminate doublets in every sample, thereby concluding the cell quality assessment phase.

2.3 Single-Cell Data Annotation, Clustering, and Dimensionality Reduction

A global normalization technique referred to as LogNormalize was utilized, which modifies the expression level in every cell to 10,000 through the use of a scaling factor (s0) and subsequent logarithmic normalization. The calculation of the cell cycle score was conducted using CellCycleScoring, and we identified Variable Features to locate genes exhibiting significant variability. To address variations in gene expression associated with mitochondrial gene proportions, ribosomal gene activity, and distinct phases of the cell cycle, we utilized the ScaleData function. For the linear reduction of dimensionality in the expression data, we utilized the RunPCA function, enabling the extraction of principal components for subsequent analysis. Batch effects were reduced using Harmony, while the RunUMAP function facilitated nonlinear dimensionality reduction, which contributed to the process of unified manifold approximation and projection. In our study on cell annotation, we focused primarily on utilizing two key resources: the CellMarker and PanglaoDB databases. These extensive databases act as vital hubs of information, detailing different cell types along with their unique marker genes. To boost the credibility of our findings, we conducted thorough literature reviews, which provided additional context and a deeper grasp of the characteristics of the cell types under investigation. Furthermore, we employed the SingleR software as an automated annotation tool, which aided in accurately identifying cell types and their associated marker genes within the specific tissues we examined. This diverse strategy enabled us to attain a broader insight into cell annotations within our study.

2.4 Analysis of Ligand-Receptor Interactions (CellChat)

We employed normalized datasets of single-cell expressions as our main input. The cellular subtypes, obtained from single-cell analysis, offered specific details that were distinctive to each type of cell. We investigated the interactions between cells, assessing both the intensity of these interactions (weights) and their occurrence (counts) to understand the dynamics of the interaction relationships. This study

provided important understanding regarding the functions and effects of different cell types concerning the disease.

2.5 SCENIC Analysis

Using the GENIE3 algorithm, the SCENIC methodology first identifies transcription factor-associated co-expression modules, then performs motif enrichment analysis on each module. We retained motifs that were significantly enriched and carried out transcription factor (TF) annotation for these motifs using a suitable database. The findings derived from the annotation were divided into two categories: those exhibiting high levels of reliability and those demonstrating low levels of reliability. TFs that were directly identified from databases, as well as those deduced from homologous genes, are classified as highly reliable, while TFs annotated solely based on motif sequence similarity are viewed as less reliable. Conserved motif analysis of co-expression module genes identified high-scoring candidates with functionally enriched motifs in TSS-proximal regulatory regions. Genes within the co-expression module that exhibited low motif scores were excluded, leading to the formation of a remaining gene set referred to as a regulatory unit (regulon). Each regulon comprises a transcription factor along with a gene set that directly impacts target genes. In the next phase of SCENIC, the activity of each regulon is evaluated across different cells. This evaluation is based on gene expression levels, which suggests that an increase in fraction indicates a higher activation level of gene concentration. This activity matrix can be used to distinguish different types and conditions of cells.

2.6 Random Survival Forest Method

The $r\ \text{and}\ omF\ \text{or}\ estSRC$ package was utilized to apply the Random Survival Forest method. This strategy aimed to assist in identifying feature genes and assessing the importance of genes linked to prognosis, conducting 1000 iterations throughout the Monte Carlo simulation (nrep = 1000). Genes exhibiting a relative importance greater than 0.1 were identified as key feature genes.

2.7 Examination of Immune Cell Infiltration

Employing the CIBERSORT algorithm, we meticulously analyzed patient data with a focus on the relative distributions of 22 specific immune cell types. This sophisticated approach allowed for a detailed examination of the immune landscape within the patient samples. Following this initial analysis, we conducted a correlation assessment to investigate the relationships between the levels of gene expression and the quantities of the identified immune cell types. By doing so, we aimed to uncover insights into how gene expression might influence or correlate with the immune profile present in the patients.

2.8 Gene Set Enrichment Analysis (GSEA)

GSEA is a commonly used method for detecting the biological significance of different disease types. The grouping of these subtypes depends on the expression levels of key genes, which helps distinguish between high and low expression categories. Subsequently, a gene set enrichment analysis was conducted to explore the differences in signaling pathways linked to the two identified groups. For this

analysis, the background gene set was sourced from version 7.0 of the annotated gene collections accessible in the MsigDB database, focusing specifically on pathways pertinent to various subtypes. A comparative analysis of differential expression was performed among the groups, focusing on gene sets that displayed notable enrichment (adjusted p-value < 0.05) according to their consistency scores.

2.9 Gene Set Variation Analysis (GSVA)

GSVA uses many genes from the molecular signature database to evaluate a comprehensive review of a single gene set. This analytical approach was utilized to evaluate possible alterations in biological functions among various samples.

2.10 Pseudotime Analysis

Monocle was applied to execute a method for sequencing single cells in pseudotime. This approach makes use of the asynchronous actions of separate cells to chart their paths in a way that mirrors biological processes, such as cell differentiation.

2.11 Tissue Samples

Between 2024 and 2025, patients undergoing surgical procedures at the Affiliated Hospital of Guangdong Medical University contributed five specimens of HCC tissues, which also comprised adjacent tumor tissues. It is noteworthy that none of these patients had undergone chemotherapy or radiation treatment prior to their surgical interventions. To maintain the integrity of the samples, these specimens were preserved in liquid nitrogen. This study received approval from the Ethics Committee at the Affiliated Hospital of Guangdong Medical University, and importantly, all patients participating in the research granted informed consent prior to their involvement in the study.

2.12 Cell Culture Maintenance and Transfection Procedures

The HCC-LM3 and Huh7 cell lines were sourced from iCell Bioscience Inc. They were cultured in Dulbecco's Modified Eagle Medium (DMEM) from Gibco, which was supplemented with 10% fetal bovine serum (FBS) and 1% penicillin-streptomycin, also supplied by Gibco. Simultaneously, human mesenchymal stem cells (hMSCs) were extracted and then grown in a medium that also included 10% FBS and 1% penicillin-streptomycin. To promote bone development, these hMSCs were maintained in a specific medium formulated to trigger osteogenesis, which was supplemented with β-glycerophosphate, vitamin C, and dexamethasone. Throughout the entire culturing process, cells were maintained in a humidified incubator set to 37°C with an atmosphere of 5% CO_2 to ensure optimal growth conditions. To investigate the role of APLP2, siRNA specifically designed to target APLP2 was procured from GenePharma, a reputable company based in China. Transient transfection was conducted on the HCC-LM3 and Huh7 cell lines in accordance with the manufacturer's guidelines for use. Aiming to further examine cellular interactions, the transfected cells were co-cultured with osteoblasts within a co-culture chamber after a 24-hour period, allowing for the observation of potential effects of the transfection on cellular behavior and interactions.

2.13 Extraction of Total RNA and Quantification via RT-qPCR

RNA was isolated from the tissues and cells impacted by HCC using the Trizol reagent supplied by Invitrogen. This extraction process was carried out following the specific protocols outlined by the manufacturer, ensuring that the procedure adhered to the recommended guidelines for optimal RNA isolation. cDNA synthesis was carried out with TAKARA reagents, followed by RT-qPCR using either the ABI QS6P or ABI 7500 systems. For human liver cancer tissues, the 18S gene served as the internal control, while GAPDH was utilized for the liver cancer cell analysis. The primer sequences utilized in the experiments are outlined in Supplement Table 1. Every sample underwent testing a minimum of three times, and the outcomes were evaluated employing the $2^{-\Delta\Delta}$CT method.

2.14 Cell Counting Kit-8 Assay (CCK-8)

Utilizing the kit from Beyotime, the CCK-8 assay required the placement of 2,000 cells in every well of a 96-well plate, then adding 100 µL of culture medium. After a 48-hour incubation period, 10 µL of CCK-8 reagent was introduced into every well, followed by an additional incubation at 37°C for one hour. Cell viability was assessed by measuring the absorbance at a wavelength of 450 nm.

2.15 Colony Formation Assay

In experiments involving cell colonies, six well plates were inoculated with 1000 cells and then incubated at 37°C for a duration of fourteen days. Following this incubation period, the cells were fixed by exposure to 4% paraformaldehyde for thirty minutes, after which they underwent staining with 0.1% crystal violet. The colonies obtained were subsequently photographed and quantified for further analysis.

2.16 Wound Healing Assay

Following the transfection of the cells, they were subsequently transferred into 6-well plates. When the confluency approached approximately 90%, a scratch was created with a 1 mL pipette tip. PBS was utilized to remove the suspended cells, allowing the remaining cells to be cultivated in a serum-free medium. Observations of wound closure occurred at 0, 24, and 48 hours with the help of an inverted microscope, while ImageJ software was utilized to quantify cell migration.

2.17 Flow Cytometry Assay

Following a treatment period of 48 hours, the cells were gathered, rinsed, and then resuspended in tubes designated for flow cytometry. Based on the guidelines given by the manufacturer (BD Biosciences), the required reagents were administered to the cells for a duration of 30 minutes prior to the commencement of the analysis.

2.18 Alizarin Red S Staining (ARS)

Human mesenchymal stem cells were cultured in a medium specifically formulated to induce osteogenesis for a period ranging from 14 to 21 days. Following this incubation phase, the cells were subjected to a treatment using 4% paraformaldehyde for a duration of 30 minutes. This treatment is crucial for fixing the cells, thereby preserving their structural integrity for subsequent analysis. After the treatment, the cells were rinsed three times with PBS. Then, they were treated with a 2% Alizarin Red S solution (Beyotime) at room temperature for a duration of 10 minutes, followed by three more rinses. The mineralized nodules that developed were examined under a microscope.

2.19 Analysis via Western Blot (WB)

For the extraction of cellular proteins, a RIPA lysis buffer was employed. The collected samples were subsequently isolated through 10% sodium dodecyl sulfate polyacrylamide gel electrophoresis. Following this procedure, the proteins are transferred to a polyvinylidene fluoride membrane. The membrane was treated using a blocking solution comprising 5% non-fat dry milk. This blocking procedure was performed for one hour at room temperature to inhibit non-specific binding of antibodies. Subsequently, the membrane was permitted to incubate at 4°C overnight in the presence of a primary antibody, promoting effective interaction with the target proteins. Following the incubation phase, a secondary antibody linked to horseradish peroxidase was introduced to the membrane and allowed to interact for one hour at ambient temperature. The primary antibodies used in this process specifically targeted APLP2 (ab140624; Abcam) and β-actin (66009-1-lg; Proteintech), ensuring accurate detection and quantification of the proteins of interest.

2.20 Examination of Statistical Information

Statistical analyses were conducted with the use of GraphPad Prism 8.0 and ImageJ software to guarantee a comprehensive evaluation of the data. In the analysis of group comparisons, especially when evaluating pairs, the primary analytical method utilized was the Student's t-test. Additionally, for the assessment of single-cell data, the R programming language, specifically version 4.3.0, was employed to facilitate this part of the analysis. To evaluate statistical significance, the determination of the PV value threshold was less than 0.05, indicating that the results were statistically significant than that level.

3. Results

3.1 Recognition of Cell Categories and Clustering at the Individual Cell Level

Figure S1 presents the metrics used for quality control in single-cell datasets. After applying UMAP for dimensionality reduction, the dataset was categorized into 16 distinct cell subpopulations (Fig. 1A). These subpopulations were further classified into nine main cell types: endothelial cells, T cells, natural killer (NK) cells, macrophages, hepatocytes, monocytes, neutrophils, B cells, and hepatic stellate cells (Fig. 1B). Moreover, the representative markers linked to these cell types are detailed in Fig. 1C, along with their proportional distributions depicted in Fig. 1D.

3.2 Assessment of Bone Metabolism and Pathway Activity

Quantification of bone metabolism was conducted using a curated selection of 288 genes from the GeneCards database. Single-cell AUCell scoring indicated that hepatocytes displayed the most notable differences in bone metabolism activity when comparing the control and disease groups (Fig. 2A), which led to their selection for further study. We then utilized the msigdbr package to retrieve the human hallmark gene set, assessed the hallmark activity of each gene set pertaining to the pathways, and applied the Average Heatmap function from the scRNAtoolVis package to create a heatmap that represents the relationship between cells and pathways (Fig. 2B). Enhanced activity in pathways linked to adipogenesis, bile acid metabolism, oxidative phosphorylation, pancreatic beta cell function, and peroxisome-related processes was observed in hepatocytes.

3.3 Differential Gene Expression in Hepatocytes and CellChat Assessment

This section explores all genes found in hepatocytes, categorizing them into two separate groups according to their scores related to bone metabolism activity: those with high activity and those with low activity. By applying the Find Markers function from the Seurat package, we identified all marker genes, omitting any that exhibited less than 10% expression across the cell population. Following this, we created a volcano plot featuring the remaining genes (Fig. 2C). The criteria for selection were as follows: $p_val_adj < 0.05$ and $avg_log2FC > 0.585$, which led to the discovery of 71 marker genes for subsequent analysis. Additionally, the CellChat analysis unveiled intricate interaction networks among the nine cell types (Fig. 3A), with a specific emphasis on hepatocyte-centered interactions and relevant pathways (Fig. 3B).

3.4 Random Survival Forest Analysis

The assessment of transcriptional regulatory networks using SCENIC highlighted ten key transcription factors associated with hepatocellular carcinoma: JUN, JUND, NFIC, ATF3, FOSB, RUNX3, REL, ETS1, and JUNB (Fig. S2). By applying random survival forest analysis to the 71 marker genes, we found genes with relative importance scores exceeding 0.1, resulting in a ranked list of 12 genes (Fig. 4A). Subsequent survival analyses demonstrated that seven of these genes showed statistically significant prognostic value (Fig. 4B-H): APLP2, SERPINC1, CAT, PDIA6, SLC2A2, C1S, and CFB. These genes have been identified as primary targets for further investigation.

3.5 Immune Infiltration and Immunoregulatory Factors

A variety of analytical approaches were utilized to thoroughly characterize the patterns of immune infiltration and the interactions among different immune cell types (Fig. 5A-C). In contrast to control samples, specimens from hepatocellular carcinoma demonstrated significantly higher quantities of memory B cells, resting dendritic cells, M0 macrophages, resting mast cells, and regulatory T cells. On

the other hand, there was a decline in the amounts of naive B cells, M2 macrophages, activated mast cells, monocytes, resting NK cells, neutrophils, plasma cells, and gamma delta T cells. Research has also been performed regarding the link between seven crucial genes and the infiltration of immune cells (Fig. 5D). Furthermore, studies were carried out to investigate the associations between these important genes and diverse immunoregulatory elements, which included both immunosuppressive and immunostimulatory factors, as well as a variety of chemokines and their related receptors (Fig. 6). These results establish hub genes as pivotal regulators of immune infiltration dynamics, functionally remodeling the cancer immune microenvironment.

3.6 Signaling Pathways Related to Essential Genes

To clarify the molecular processes by which essential genes affect disease progression, analyses were performed using both GSEA and GSVA methods. The results from GSEA uncovered distinct pathway associations linked to each essential gene.

- APLP2: significantly enriched in focal adhesion, leukocyte transendothelial migration, and Hedgehog signaling pathways (Fig. 7A);
- SERPINC1: enriched in Hippo signaling, Wnt signaling, and osteoclast differentiation pathways (Fig. 7B);
- CAT: associated with cell cycle regulation, thermogenesis, and Hippo signaling (Fig. 7C);
- PDIA6: involved in muscle cell cytoskeleton organization, mineral absorption, and osteoclast differentiation (Fig. 7D);
- SLC2A2: enriched in PPAR signaling, lysosomal function, and cholesterol metabolism pathways (Fig. 7E);
- C1S: demonstrated involvement in PPAR signaling, Hippo signaling, and Wnt signaling (Fig. 7F);
- CFB: associated with AMPK signaling, FoxO signaling, and PPAR signaling pathways (Fig. 7G).

The GSVA analysis provided additional insights, indicating that:

- The APLP2 protein interacts with the WNT/β-catenin signaling pathway as well as the PI3K-AKT-mTOR signaling cascade (Fig. 8A).;
- SERPINC1 is connected with both the early and late estrogen response pathways (Fig. 8B);
- CAT participates in the inflammatory response as well as the initial estrogen response (Fig. 8C);
- PDIA6 is involved in the signaling pathways of both WNT/β-catenin and PI3K-AKT-mTOR (Fig. 8D);
- SLC2A2 is related to the late and early responses to estrogen (Fig. 8E);
- C1S is similarly connected to both late and early responses to estrogen (Fig. 8F);
- CFB modulates WNT/β-catenin signaling while mediating primary estrogen response initiation (Fig. 8G).

The findings indicate that the key genes identified could affect the progression of the disease by altering crucial signaling pathways.

3.7 Analysis of Single-Cell Expression and Pseudotemporal Trajectories

To study the most important gene expression profiles at each cell level, we used the viewing feature provided by the Seurat software package. This involved the application of the DotPlot and FeaturePlot functions (Fig. 9). These tools enable a detailed representation of gene expression, allowing for a better understanding of the spatial distribution and variations in gene activity across individual cells.

Subsequently, an investigation into pseudotemporal trajectories was conducted using the Monocle package. The results indicated that cells in the control group were predominantly found in the later stages of differentiation, while cells from the disease group were observed at various points, including the early, intermediate, and advanced stages of differentiation (Fig. 10A-C). Genes exhibiting the most significant changes throughout the pseudotime were selected for visualization. The horizontal axis represents pseudotime, while gene expression profiles are illustrated on the vertical axis, where they have been automatically categorized into three distinct clusters. Notably, genes like TXN, HINT1, and RPS13 were mainly expressed during the earlier stages of differentiation, unlike NEAT1, HELLPAR, and POLE, which were more active in the later stages (Fig. 10D). Moreover, modifications in the expression levels of essential genes throughout the differentiation pathways were illustrated (Fig. 10E).

3.8 Network of Co-expression Among Genes Involved in Bone Metabolism Genes

Sourced from the GeneCards database (https://www.genecards.org/), genes related to bone metabolism were analyzed through correlation studies alongside the seven crucial genes according to their relevance scores. The resultant co-expression network highlighted the following findings:

- A positive correlation has been detected between APLP2 and SQSTM1(r = -0.31; Fig. S3);
- An inverse relationship was identified for C1S and RTEL1(r = -0.55; Fig. S4);
- CAT revealed a negative relationship with COL1A1(r = -0.44; Fig. S5);
- CFB showed a negative association with RTEL1(r = -0.54; Fig. S6);
- PDIA6 was noted to have a negative relationship with RTEL1(r = -0.32; Fig. S7);
- SERPINC1 exhibited a negative correlation with RTEL1(r = -0.45; Fig. S8);
- SLC2A2 demonstrated the strongest negative correlation with RTEL1(r = -0.58; Fig. S9).

3.9 Examination of Immunometabolic Pathways

To quantitatively evaluate the scores of genes associated with immune metabolism pathways at the single-cell level, AUCell was utilized, with bubble plots offering visual representations of differences in activity. Observations indicated that the genes SERPINC1, PDIA6, SLC2A2, CFB, CAT, APLP2, and C1S exhibited enhanced activity in multiple pathways related to immune metabolism, encompassing coagulation, peroxisomal metabolism, adipogenesis, bile acid metabolism, oxidative phosphorylation, and the metabolism of xenobiotics (Fig. S10).

3.10 In Vitro Analysis of APLP2's Role as a Contributing Factor in HCC and Its Impact on Bone Metabolism

Quantitative PCR analysis was performed on HCC tissues from five different patient groups to evaluate the expression of seven essential genes: APLP2, SERPINC1, CAT, PDIA6, SLC2A2, C1S, and CFB. The findings demonstrate that the expression levels of APLP2 and PDIA6 in tissues affected by HCC were considerably higher than those found in nearby non-cancerous tissues, with APLP2 displaying the most pronounced increase (Fig. 11A). Prior research has indicated that tumors can modify the makeup of bone marrow and facilitate bone degradation(11). A well-known factor that plays a role in unfavorable outcomes for individuals with HCC is the urgent requirement for creating effective methods to alleviate the effects of HCC on bone metabolism(12). The investigation focused on the significant role of APLP2 as an important gene in liver cancer and its impact on bone metabolism. siRNA targeting APLP2 was designed and introduced into two liver cancer cell lines: HCC-LM3 and Huh7. The evaluation of APLP2 knockdown was performed using quantitative PCR and Western blot analysis (Fig. 11B-C). To investigate the growth of cells, we conducted CCK-8 assays in conjunction with colony formation assays, which revealed that lower levels of APLP2 led to a significant reduction in the proliferation of liver cancer cells (Fig. 11D-E). Furthermore, diminished APLP2 levels were shown to hinder the migratory capacity of liver cancer cells, as indicated by wound healing assays (Fig. 11F). Flow cytometry analysis revealed that APLP2 knockdown resulted in increased rates of apoptosis among liver cancer cells (Fig. 11G). These in vitro findings support the hypothesis that APLP2 exhibits oncogenic characteristics in liver cancer. Additionally, liver cancer cells were co-cultured with osteoblasts to examine the influence of APLP2 on bone metabolism (Fig. 11H). ARS staining demonstrated that liver cancer cells inhibited osteoblast differentiation; however, knocking down APLP2 counteracted this inhibition (Fig. 11I). The qPCR results were consistent with the staining findings (Fig. 11J). Overall, these findings support the notion that APLP2 is involved in HCC, indicating that inhibiting it could potentially reduce the negative impact of HCC on bone metabolism.

4. Discussion

HCC is a prevalent form of cancer that significantly contributes to global cancer-related mortality rates(17). The rates of incidence and mortality associated with HCC have shown a consistent rise, with a majority of patients receiving diagnoses at advanced stages of the illness, leading to poor prognoses. Currently, the primary curative methods for HCC include the surgical excision of the tumor and liver transplantation; nonetheless, their application is limited(2, 18, 19). Strong clinical research evidence

indicates that the profile of immune cell types within HCC tumors is significantly linked to patient outcomes and responses to treatment(20–22). Cells within the immune system are significant contributors to tumor microenvironments(23, 24), acting as crucial mediators in cancer advancement and therapeutic results while also affecting immunotherapy responses across various cancer forms(25–27). The composition of immune cells within the cancer microenvironment plays a vital role in categorizing HCC into three distinct immune subtypes. These subtypes—high, medium, and low—vary in the extent of immune cell presence and their activity levels. Understanding the varying makeup of immune cells is essential for grasping the immune landscape in HCC, which has significant implications for developing targeted therapies and treatment strategies. Identified by a notable abundance of T cells along with a rise in B cells and plasma cells, the Immune-high subtype acts as an independent positive prognostic marker related to B cells(28, 29). Consequently, emphasizing the immune variability associated with HCC could signify a potentially beneficial treatment strategy.

Recent breakthroughs in oncology have garnered substantial interest in therapies that harness the immune system, particularly ICIs. These novel treatments have demonstrated considerable potential in boosting the body's inherent capacity to fight cancer. An expanding collection of studies underscores that blocking immune checkpoints, especially the PD-1/PD-L1 and CTLA-4 pathways, is critical for enhancing results in patients with HCC. By effectively blocking these checkpoints, ICIs facilitate the reactivation of adaptive immune responses, thereby significantly improving the prognosis for individuals diagnosed with this challenging form of cancer(30–32). Despite its novelty, ICI therapy benefits only a limited subgroup of HCC patients and is frequently associated with immune-related toxicities(30, 33, 34). Consequently, it is essential to create strategies that enhance their efficacy, encompassing approaches for patient stratification, biomarker-guided treatments, and the thoughtful choice of combination therapies.

A combined methodology using scRNA-seq and transcriptomics was employed to investigate the cellular diversity found in HCC, its implications for bone metabolism, and possible therapeutic targets. Within the microenvironment of HCC, researchers identified and characterized nine unique populations of cells: endothelial cells, T lymphocytes, natural killer (NK) cells, macrophages, hepatocytes, monocytes, neutrophils, B lymphocytes, and hepatic stellate cells. Notably, hepatocytes exhibited the most pronounced variations in scores related to bone metabolism. Furthermore, ten key transcription factors linked to the pathogenesis of HCC were identified, including JUN, JUND, NFIC, ATF3, FOSB, RUNX3, REL, ETS1, and JUNB. In addition, seven significant genes connected to prognosis (APLP2, SERPINC1, CAT, PDIA6, SLC2A2, C1S, and CFB) were found to be significantly enriched in immune-metabolic pathways including coagulation, peroxisome activity, adipogenesis, bile acid metabolism, oxidative phosphorylation, and xenobiotic metabolism. These genetic markers displayed strong correlations with various immune cell types and immunomodulatory factors(35–41). A co-expression network was created to examine the interrelations among these prognosis-related genes and those relevant to bone metabolism. The results emphasize the promise of these seven genes as therapeutic candidates for HCC. From a mechanistic angle, targeting these genes could allow for a simultaneous impact on

immune responses and bone metabolism, thereby presenting a dual therapeutic approach to combat HCC progression and its systemic effects.

Research conducted *in vivo* has demonstrated a significant difference in the expression levels of APLP2 when comparing HCC tissues to the surrounding normal tissues. This finding highlights the altered regulation of APLP2 in the context of HCC, suggesting its potential role in the pathology of the disease. The significant variations noted in expression levels might also suggest that APLP2 has the potential to function as an important biomarker for distinguishing cancerous liver tissues from their non-cancerous counterparts, providing valuable insights into the fundamental mechanisms driving tumor progression. This alteration in expression signifies a potential biomarker for HCC progression. Furthermore, the deliberate reduction of APLP2 expression has been shown to have a profound effect on multiple cellular processes within HCC cells. This reduction greatly impedes the growth, migration, and infiltration of cells, which are all crucial components in the progression of cancer. Moreover, the diminished expression of APLP2 enhances apoptosis, suggesting that focusing on APLP2 could represent a potential therapeutic strategy to elevate the mortality rate of HCC cells(42, 43). Co-culture experiments demonstrated that HCC cells inhibited the osteogenic differentiation of osteoblasts, an effect that was reversed after the knockdown of APLP2. The results underline the significant role of APLP2 in the advancement of tumors and its potential use as a therapeutic target to affect antitumor immunity and bone metabolism.

Nonetheless, a few limitations exist in this study. Firstly, the research was solely concentrated on in vitro assessments regarding the interaction between HCC cells and osteoblasts, thereby lacking mechanistic insights into how APLP2 influences antitumor immunity. Future research utilizing animal models is necessary to address this issue. Moreover, different levels of PDIA6 expression were observed in HCC tissues, highlighting the necessity for additional investigation into its role in tumor progression.

5. Conclusion

To conclude, this research employs scRNA-seq alongside transcriptome analysis to explore differences in HCC, their impact on bone metabolism, and the detection of relevant therapeutic targets. A total of seven key candidate genes were identified, and functional validation confirmed the dual role of APLP2 in tumor suppression and bone metabolism regulation. The findings indicate a possible translational strategy aimed at increasing the effectiveness of treatment and boosting survival rates for individuals with HCC.

Abbreviations

HCC: Hepatocellular Carcinoma; PD-1: Programmed cell death-1; PD-L1: Programmed cell death ligand 1; scRNA-seq: single-cell RNA sequencing; GEO: Gene Expression Omnibus; TCGA: The Cancer Genome Atlas; MAD: Median Absolute Deviation; SCENIC: single-cell regulatory network inference and clustering; siRNA: Short Interfering RNA; RT-qPCR: RNA extraction and quantitative real-time polymerase chain

reaction; CCK8: Cell Counting Kit-8 assay; ARS: Alizarin Red S Staining; ALP: Alkaline Phosphatase Staining; GSEA: Gene Set Enrichment Analysis; GSVA: Gene Set Variation Analysis; hMSCs: Human Mesenchymal Stem Cells; ICIs: Immune Checkpoint Inhibitors.

Declarations

Ethics approval and consent to participate

This study involving human participants was approved by the Ethics Committee of the Affiliated Hospital of Guangdong Medical University (Approval ID: **YJYS2024240**; Date: **May 8, 2024**). Written informed consent was obtained from all participants prior to tissue collection.

Consent for publication

Not applicable. This manuscript contains no individual person's data, images, or videos requiring consent for publication.

Availability of data and materials

The single-cell RNA sequencing dataset (GSE223204) analyzed during this study is publicly available in the Gene Expression Omnibus (GEO) repository at https://www.ncbi.nlm.nih.gov/geo/info/datasets.html.

The bulk transcriptomic dataset (TCGA-LIHC) is available from The Cancer Genome Atlas (TCGA) portal at https:// portal.gdc.cancer.gov/.

Additional data generated during this study (including qPCR validation and functional assay results) are available from the corresponding authors upon reasonable request.

Competing interests

The authors declare that they have no competing interests, financial or non-financial, related to this work.

Funding

This work was supported by:

- Guangdong Medical Science and Technology Research Fund Project (B2024006)
- Scientific research project of Guangdong Provincial Administration of Traditional Chinese Medicine (20251205, 20261199)
- Guangdong Higher Education Association's "14th Five Year Plan" 2024 Higher Education Research Project (24GQN06)
- Zhanjiang Science and Technology Development Special Fund (2022A01176)
- The high-level talents scientific research start-up funds of the Affliated Hospital of Guangdong Medical University (GCC2022008, GCC2024022)

- Affiliated Hospital of Guangdong Medical University Clinical Research Program(LCYJ2019B012)
- Special Project for Clinical and Basic Sci&Tech Innovation of Guangdong Medical University(GDMULCJC2025049, GDMULCJC2025063)
- National Natural Science Foundation of China (82272505, 82472454, 81874000)
- Natural Science Foundation of Guangdong Province (2023A1515011040)
- Research Grants Council of Hong Kong (14119124, 14113723, 14121721, N_CUHK472/22, T13-402/17-N, AoE/M-402/20)

Funders had no role in study design, data collection/analysis, or manuscript preparation.

Authors' contributions

Z.L., J.Z. and Z.S. contributed equally to this work. Conceptualization, X.F. and S.L.; Methodology, Z.L., J.Z., Z.S., B.W. (Bo Wu) and C.S.; Software, Z.S. and C.S.; Validation, Z.S., H.Y., S.B. and X.W.; Formal Analysis, C.S.; Investigation, L.D. and S.C.; Resources, B.W. (Bo Wei), X.F. and S.L.; Data Curation, B.W. (Bo Wu); Writing – Original Draft Preparation, Z.L. and J.Z.; Writing – Review & Editing, X.F. and S.L.; Visualization, S.C.; Supervision, B.W. (Bo Wei), X.F. and S.L.; Project Administration, X.F. and S.L.; Funding Acquisition, Z.L., B.W. (Bo Wei) and S.L. All authors have read and agreed to the published version of the manuscript.

Acknowledgements

We thank the clinicians and pathologists at the Affiliated Hospital of Guangdong Medical University for sample collection support. We also acknowledge the technical assistance from the Core Facility of Macau University of Science and Technology. Professional editing services were not utilized.

References

1. Brown ZJ, Tsilimigras DI, Ruff SM, Mohseni A, Kamel IR, Cloyd JM, et al. Management of Hepatocellular Carcinoma: A Review. JAMA Surg. 2023;158(4):410–20.
2. Forner A, Reig M, Bruix J. Hepatocellular carcinoma. Lancet. 2018;391(10127):1301–14.
3. Vogel A, Meyer T, Sapisochin G, Salem R, Saborowski A. Hepatocellular carcinoma. Lancet. 2022;400(10360):1345–62.
4. Yang W, Nguyen R, Safri F, Shiddiky MJA, Warkiani ME, George J et al. Liquid Biopsy in Hepatocellular Carcinoma: ctDNA as a Potential Biomarker for Diagnosis and Prognosis. Curr Oncol Rep. 2025.
5. Zhuang H, Tang C, Wang W, Chen B, Wang B, Hua Y et al. Sitravatinib targets TYRO3 to augment the anti-tumor immune response of PD-1 blockade in hepatocellular carcinoma. Clin Cancer Res. 2025.
6. Gu J, Bao S, Han L, Yu X, Jia Z, Huang C. Prediction of PD-1 Expression and Outcomes of Combined Therapy in Hepatocellular Carcinoma: an MRI-Based Radiomics Approach. J Imaging Inf Med. 2025.

7. Xu W, Weng J, Zhao Y, Xie P, Xu M, Liu S et al. FMO2(+) cancer-associated fibroblasts sensitize anti-PD-1 therapy in patients with hepatocellular carcinoma. J Immunother Cancer. 2025;13(5).
8. Tang P, Zhou F. Efficacy and safety of PD-1/PD-L1 inhibitors combined with tyrosine kinase inhibitors as first-line treatment for hepatocellular carcinoma: a meta-analysis and trial sequential analysis of randomized controlled trials. Front Pharmacol. 2025;16:1535444.
9. Ruiz de Galarreta M, Bresnahan E, Molina-Sanchez P, Lindblad KE, Maier B, Sia D, et al. beta-Catenin Activation Promotes Immune Escape and Resistance to Anti-PD-1 Therapy in Hepatocellular Carcinoma. Cancer Discov. 2019;9(8):1124–41.
10. Li Q, Han J, Yang Y, Chen Y. PD-1/PD-L1 checkpoint inhibitors in advanced hepatocellular carcinoma immunotherapy. Front Immunol. 2022;13:1070961.
11. Copin P, Ronot M, Vilgrain V. Hepatocellular carcinoma with osseous metaplasia and bone marrow elements. Clin Gastroenterol Hepatol. 2015;13(3):e26–7.
12. Clezardin P, Coleman R, Puppo M, Ottewell P, Bonnelye E, Paycha F, et al. Bone metastasis: mechanisms, therapies, and biomarkers. Physiol Rev. 2021;101(3):797–855.
13. Yin JJ, Pollock CB, Kelly K. Mechanisms of cancer metastasis to the bone. Cell Res. 2005;15(1):57–62.
14. Minisola S, Fukumoto S, Xia W, Corsi A, Colangelo L, Scillitani A, et al. Tumor-induced Osteomalacia: A Comprehensive Review. Endocr Rev. 2023;44(2):323–53.
15. Yang Y, Ni Q, Li H, Sun J, Zhou X, Qu L et al. Genomic and the tumor microenvironment heterogeneity in multifocal hepatocellular carcinoma. Hepatology. 2024.
16. Jin H, Kim W, Yuan M, Li X, Yang H, Li M, et al. Identification of SPP1 (+) macrophages as an immune suppressor in hepatocellular carcinoma using single-cell and bulk transcriptomics. Front Immunol. 2024;15:1446453.
17. You Y, Wen D, Zeng L, Lu J, Xiao X, Chen Y, et al. ALKBH5/MAP3K8 axis regulates PD-L1 + macrophage infiltration and promotes hepatocellular carcinoma progression. Int J Biol Sci. 2022;18(13):5001–18.
18. Clavien PA, Lesurtel M, Bossuyt PM, Gores GJ, Langer B, Perrier A et al. Recommendations for liver transplantation for hepatocellular carcinoma: an international consensus conference report. Lancet Oncol. 2012;13(1):e11-22.
19. Vitale A, Peck-Radosavljevic M, Giannini EG, Vibert E, Sieghart W, Van Poucke S, et al. Personalized treatment of patients with very early hepatocellular carcinoma. J Hepatol. 2017;66(2):412–23.
20. Yasuoka H, Asai A, Ohama H, Tsuchimoto Y, Fukunishi S, Higuchi K. Increased both PD-L1 and PD-L2 expressions on monocytes of patients with hepatocellular carcinoma was associated with a poor prognosis. Sci Rep. 2020;10(1):10377.
21. Cao D, Chen MK, Zhang QF, Zhou YF, Zhang MY, Mai SJ, et al. Identification of immunological subtypes of hepatocellular carcinoma with expression profiling of immune-modulating genes. Aging. 2020;12(12):12187–205.

22. Liu F, Qin L, Liao Z, Song J, Yuan C, Liu Y, et al. Microenvironment characterization and multi-omics signatures related to prognosis and immunotherapy response of hepatocellular carcinoma. Exp Hematol Oncol. 2020;9:10.
23. Park J, Hsueh PC, Li Z, Ho PC. Microenvironment-driven metabolic adaptations guiding CD8(+) T cell anti-tumor immunity. Immunity. 2023;56(1):32–42.
24. Maiorino L, Dassler-Plenker J, Sun L, Egeblad M. Innate Immunity and Cancer Pathophysiology. Annu Rev Pathol. 2022;17:425–57.
25. Liu Y, Xun Z, Ma K, Liang S, Li X, Zhou S, et al. Identification of a tumour immune barrier in the HCC microenvironment that determines the efficacy of immunotherapy. J Hepatol. 2023;78(4):770–82.
26. Ugel S, Cane S, De Sanctis F, Bronte V. Monocytes in the Tumor Microenvironment. Annu Rev Pathol. 2021;16:93–122.
27. Ren X, Zhang L, Zhang Y, Li Z, Siemers N, Zhang Z. Insights Gained from Single-Cell Analysis of Immune Cells in the Tumor Microenvironment. Annu Rev Immunol. 2021;39:583–609.
28. Kurebayashi Y, Ojima H, Tsujikawa H, Kubota N, Maehara J, Abe Y, et al. Landscape of immune microenvironment in hepatocellular carcinoma and its additional impact on histological and molecular classification. Hepatology. 2018;68(3):1025–41.
29. Nguyen CT, Caruso S, Maille P, Beaufrere A, Augustin J, Favre L, et al. Immune Profiling of Combined Hepatocellular- Cholangiocarcinoma Reveals Distinct Subtypes and Activation of Gene Signatures Predictive of Response to Immunotherapy. Clin Cancer Res. 2022;28(3):540–51.
30. Ruf B, Heinrich B, Greten TF. Immunobiology and immunotherapy of HCC: spotlight on innate and innate-like immune cells. Cell Mol Immunol. 2021;18(1):112–27.
31. Rimassa L, Finn RS, Sangro B. Combination immunotherapy for hepatocellular carcinoma. J Hepatol. 2023;79(2):506–15.
32. Gao X, Xu N, Li Z, Shen L, Ji K, Zheng Z, et al. Safety and antitumour activity of cadonilimab, an anti-PD-1/CTLA-4 bispecific antibody, for patients with advanced solid tumours (COMPASSION-03): a multicentre, open-label, phase 1b/2 trial. Lancet Oncol. 2023;24(10):1134–46.
33. Ramos-Casals M, Brahmer JR, Callahan MK, Flores-Chavez A, Keegan N, Khamashta MA, et al. Immune-related adverse events of checkpoint inhibitors. Nat Rev Dis Primers. 2020;6(1):38.
34. Martins F, Sofiya L, Sykiotis GP, Lamine F, Maillard M, Fraga M, et al. Adverse effects of immune-checkpoint inhibitors: epidemiology, management and surveillance. Nat Rev Clin Oncol. 2019;16(9):563–80.
35. Huang X, Yang J, Xi H, Zhang M, Oh Y, Jin Z, et al. Implication of Amyloid Precursor-like Protein 2 Expression in Cutaneous Squamous Cell Carcinoma Pathogenesis. Vivo. 2024;38(1):399–408.
36. Zhang Y, Zhang T, Yin Q, Luo H. Development and validation of genomic and epigenomic signatures associated with tumor immune microenvironment in hepatoblastoma. BMC Cancer. 2021;21(1):1156.

37. Nosalski R, Siedlinski M, Denby L, McGinnigle E, Nowak M, Cat AND, et al. T-Cell-Derived miRNA-214 Mediates Perivascular Fibrosis in Hypertension. Circ Res. 2020;126(8):988–1003.
38. Ma Y, Liu E, Fan H, Li C, Huang P, Cui M, et al. RBM47 promotes cell proliferation and immune evasion by upregulating PDIA6: a novel mechanism of pancreatic cancer progression. J Transl Med. 2024;22(1):1164.
39. van Eijck CWF, Ju J, van 't Land FR, Verheij M, Li Y, Stubbs A, et al. The tumor immune microenvironment in resected treatment-naive pancreatic cancer patients with long-term survival. Pancreatology. 2024;24(7):1057–65.
40. Zhang X, Lan R, Liu Y, Pillarisetty VG, Li D, Zhao CL, et al. Complement activation in tumor microenvironment after neoadjuvant therapy and its impact on pancreatic cancer outcomes. NPJ Precis Oncol. 2025;9(1):58.
41. Zhang S, Pang K, Feng X, Zeng Y. Transcriptomic data exploration of consensus genes and molecular mechanisms between chronic obstructive pulmonary disease and lung adenocarcinoma. Sci Rep. 2022;12(1):13214.
42. Tao Z, Huang J, Li J. Comprehensive intratumoral heterogeneity landscaping of liver hepatocellular carcinoma and discerning of APLP2 in cancer progression. Environ Toxicol. 2024;39(2):612–25.
43. Su Y, Xue C, Gu X, Wang W, Sun Y, Zhang R, et al. Identification of a novel signature based on macrophage-related marker genes to predict prognosis and immunotherapeutic effects in hepatocellular carcinoma. Front Oncol. 2023;13:1176572.

Figures

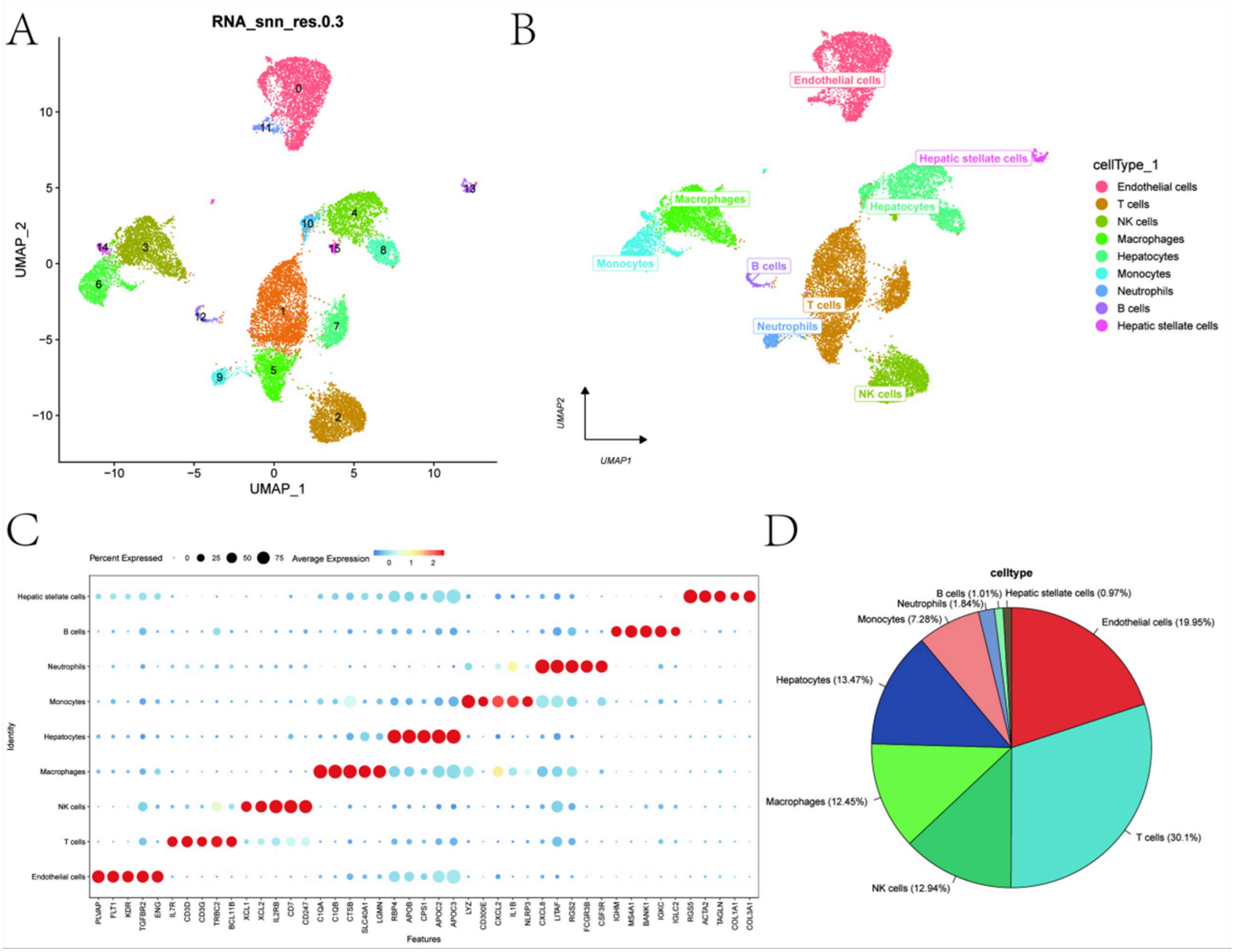


Figure 1

The cellular landscape of hepatocellular carcinoma examined at a single-cell level. (A) Following the application of UMAP for dimensionality reduction, the sample dataset was segmented into 16 unique cell subpopulations. (B) The characterization process identified nine main cell types: endothelial cells, T cells, natural killer (NK) cells, macrophages, hepatocytes, monocytes, neutrophils, B cells, and hepatic stellate cells. (C) Marker genes characteristic of each cell type are shown. (D) The relative distribution of these nine primary cell types is illustrated

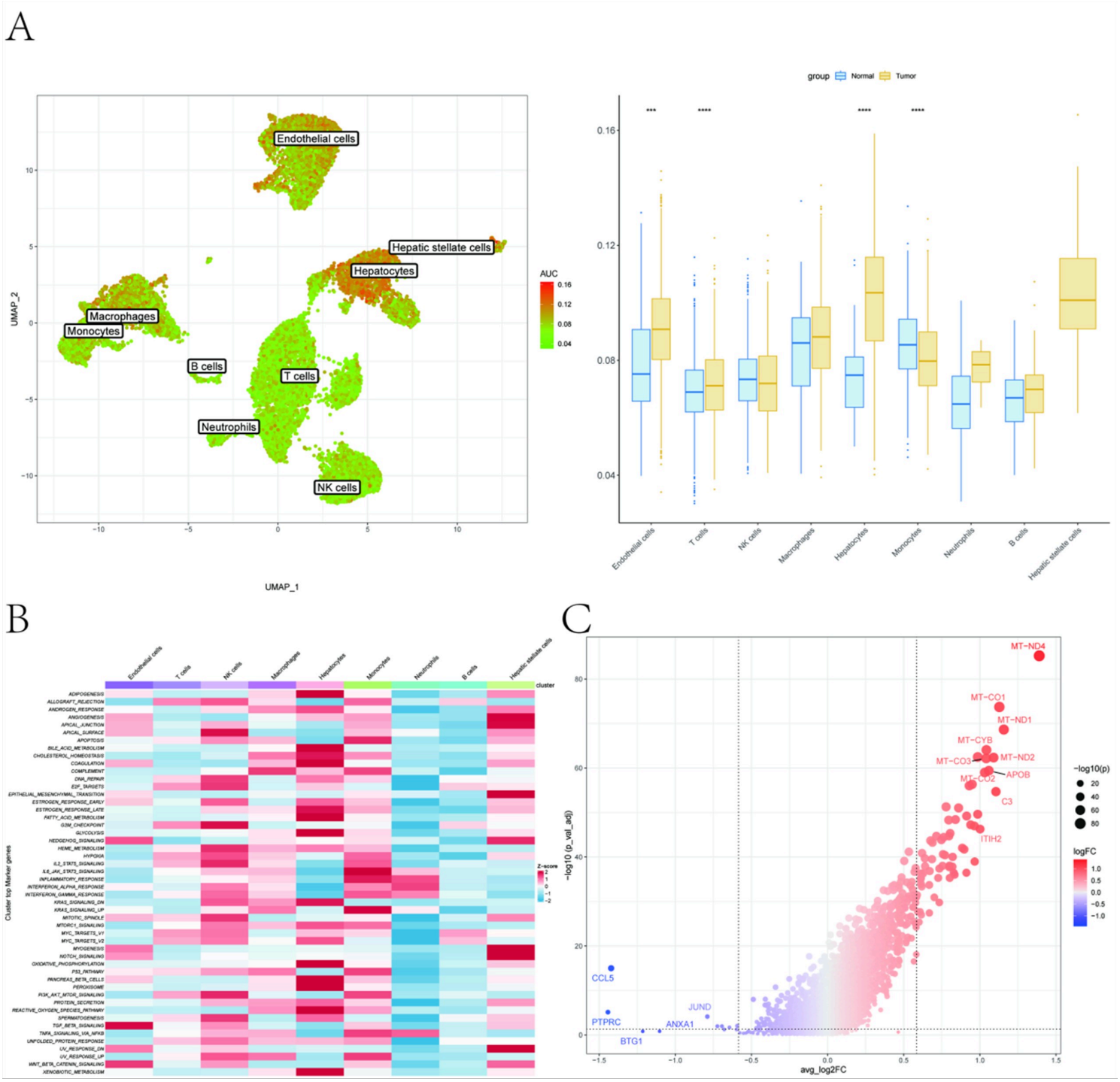


Figure 2

An in-depth analysis of single-cell transcriptomes uncovers variations in cellular diversity, functional states, and essential mechanisms for differentiation. (A) Distinctions in the metabolic activity of hepatocyte bone between control and affected groups; (B) Illustration of interactions among cells and their associated pathways; (C) Assessment of gene expression in hepatocytes categorized by high and low bone metabolism scores.

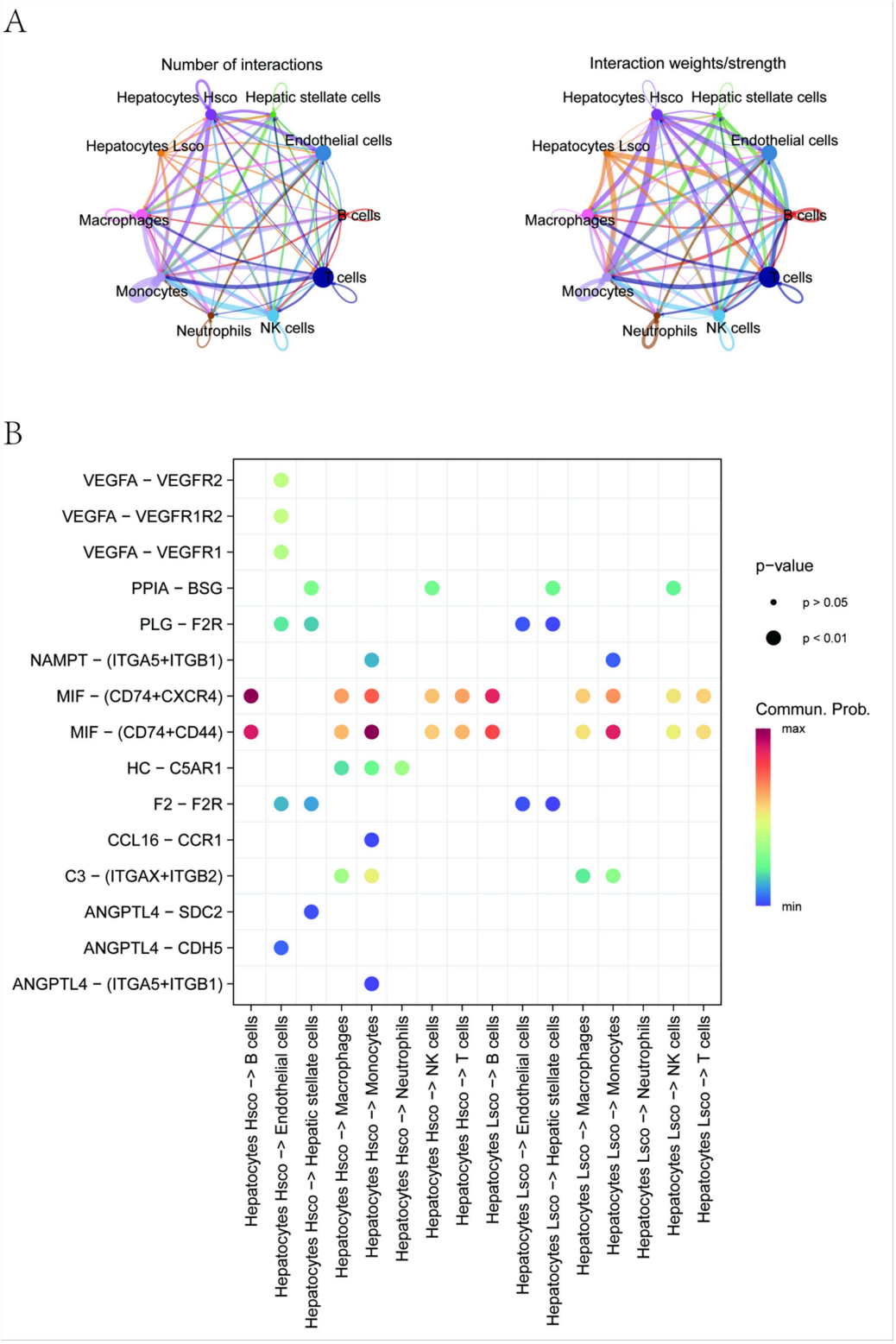


Figure 3

Cellular communication networks highlight the central signaling hub role of hepatocyte subpopulations in the tumor microenvironment. (A) Interaction network among distinct cell types; (B) Hepatocyte-centered ligand-receptor-specific interaction network.

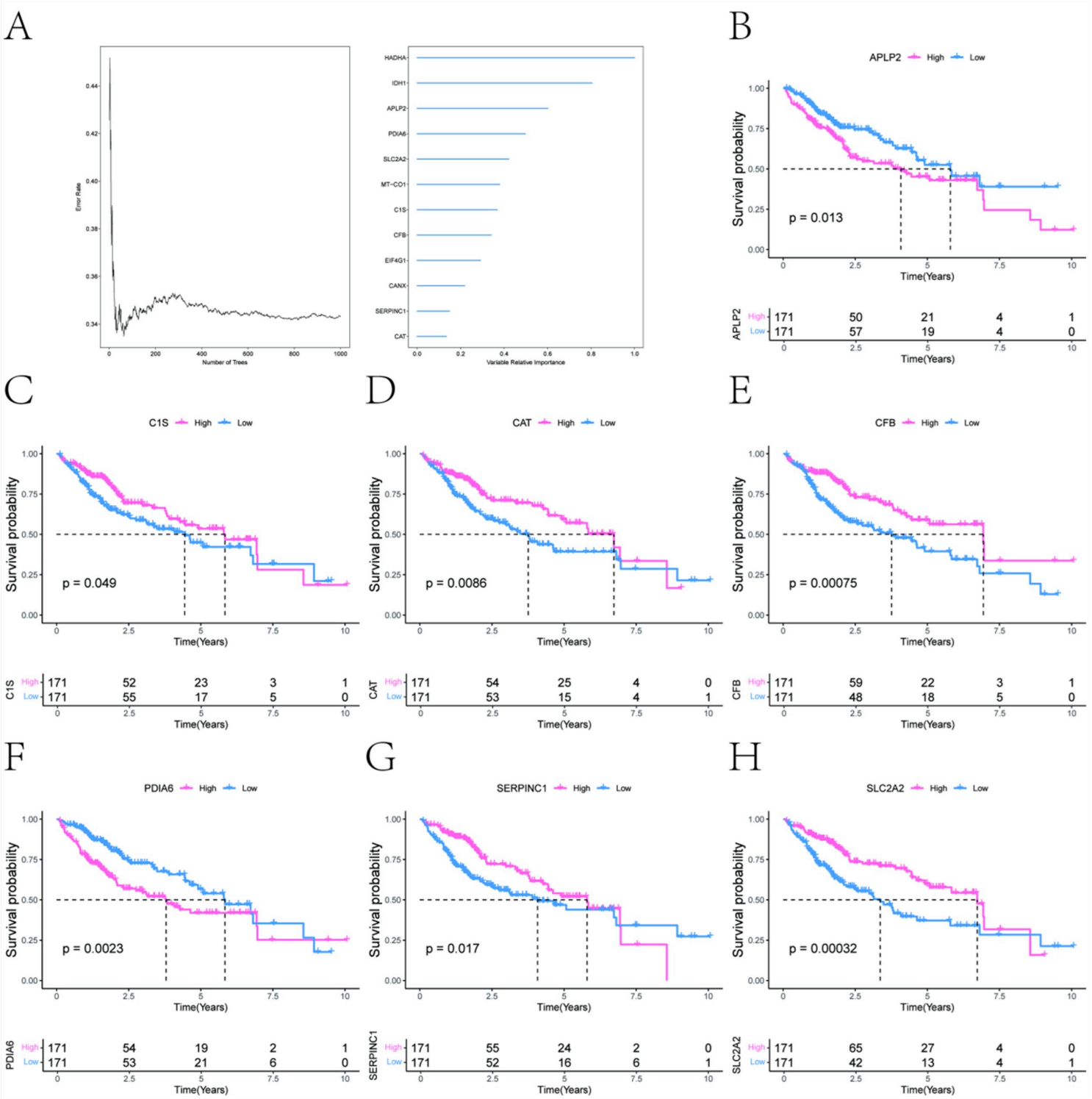


Figure 4

Machine learning-driven discovery and clinical validation of prognostic markers. (A) Survival analysis via randomized survival forests for 12 key gene signatures. (B–H) Survival analysis stratified by expression levels of seven key genes: APLP2, SERPINC1, CAT, PDIA6, SLC2A2, C1S, and CFB.

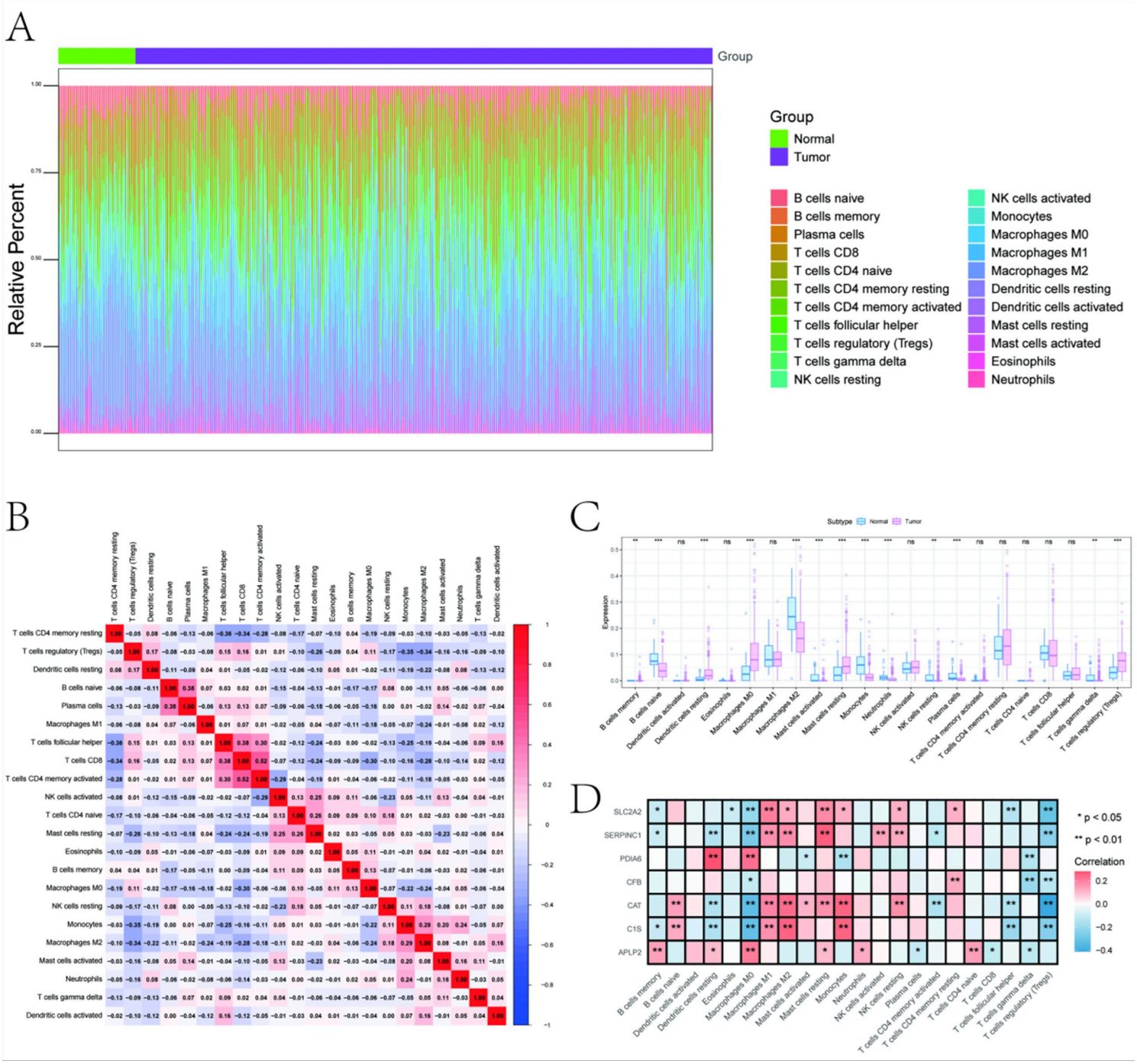


Figure 5

A thorough analysis of the tumor immune microenvironment uncovers functional relationships between prognostic markers and populations of immune cells. (A) A comparison of immune cell makeup in normal versus tumor tissues; (B) A heatmap showcasing networks of immune cell interactions; (C) Expression patterns of essential immune cell subgroups within tumor tissues; (D) Examination of the relationships between prognostic indicators and the presence of immune cells.

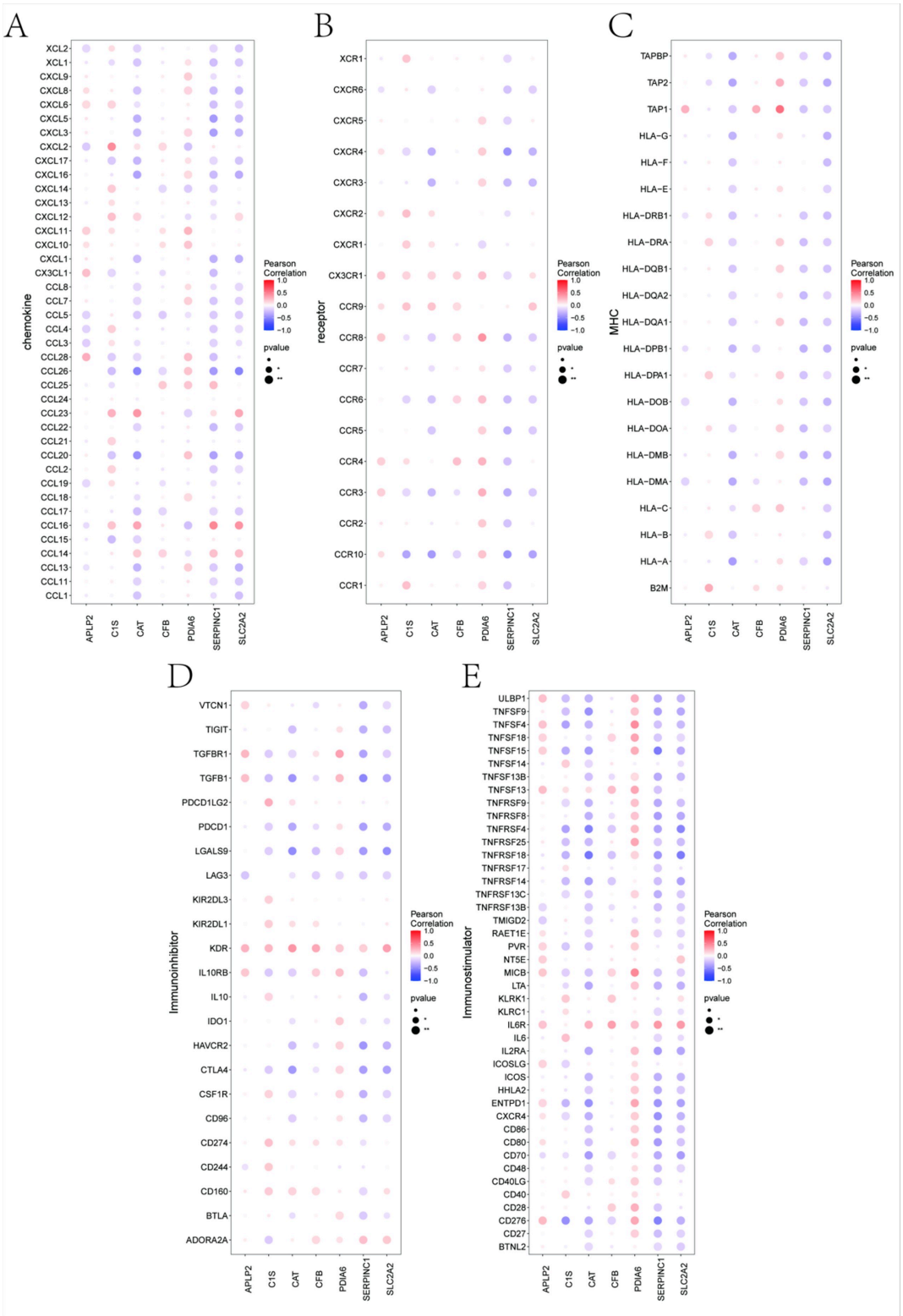


Figure 6

Investigation of Cross-Omics Relationships Concerning Prognostic Indicators and Immunoregulatory Networks. (A) Assessment of the relationship between profiles of chemokine expression and prognostic indicators. (B) Network evaluation of associations involving chemokine receptors. (C) Examination of expression relationships associated with MHC molecules. (D) Exploration of connections among immunosuppressive checkpoints. (E) Study of interactions pertaining to immunostimulatory molecules.

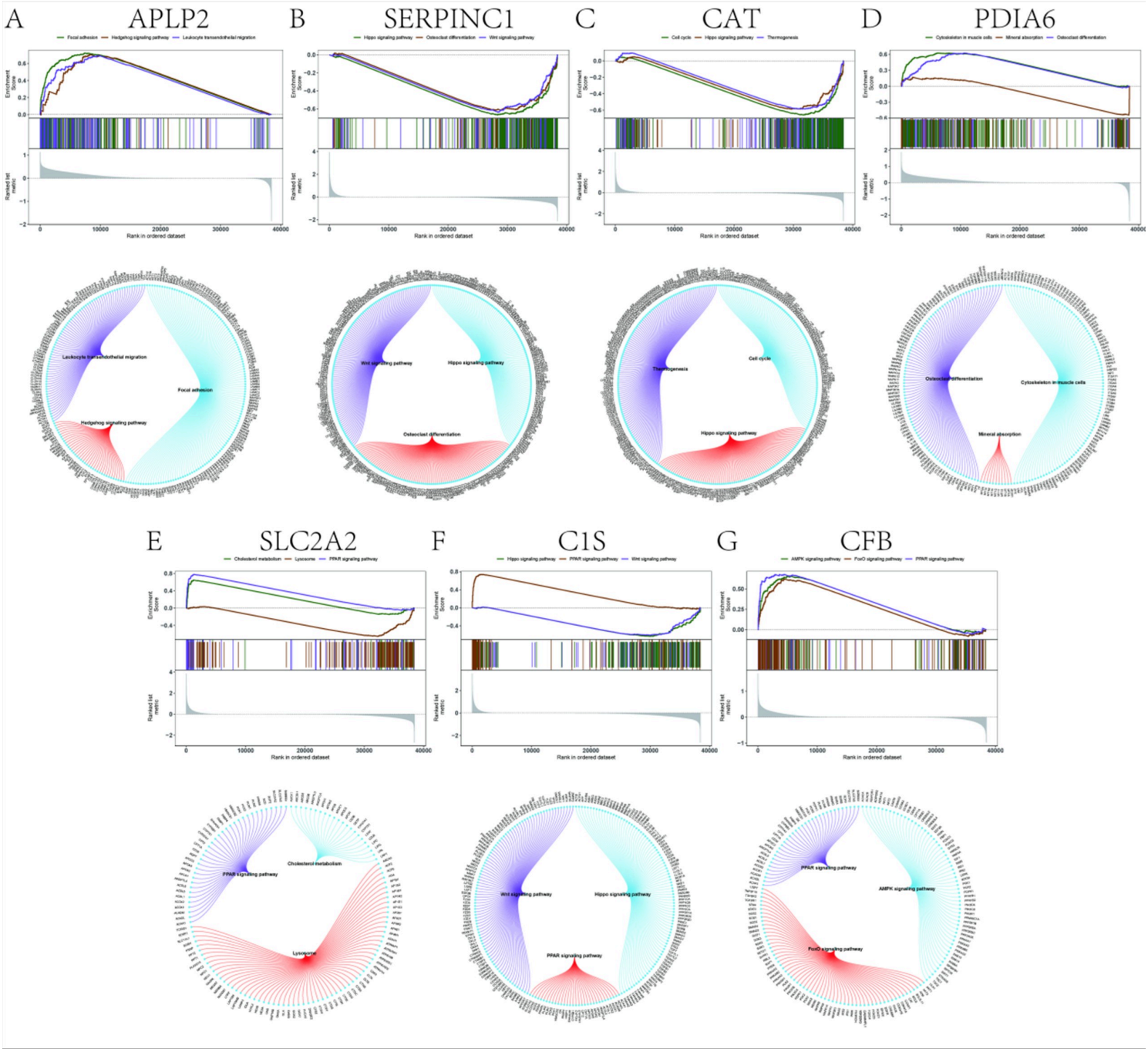


Figure 7

Examination of Pathway Enrichment Associated with Significant Prognostic Indicators. (A) APLP2; (B) SERPING1; (C) CAT; (D) PDIA6; (E) SLC2A2; (F) C1S; (G) CFB: GSEA and pathway enrichment assessment.

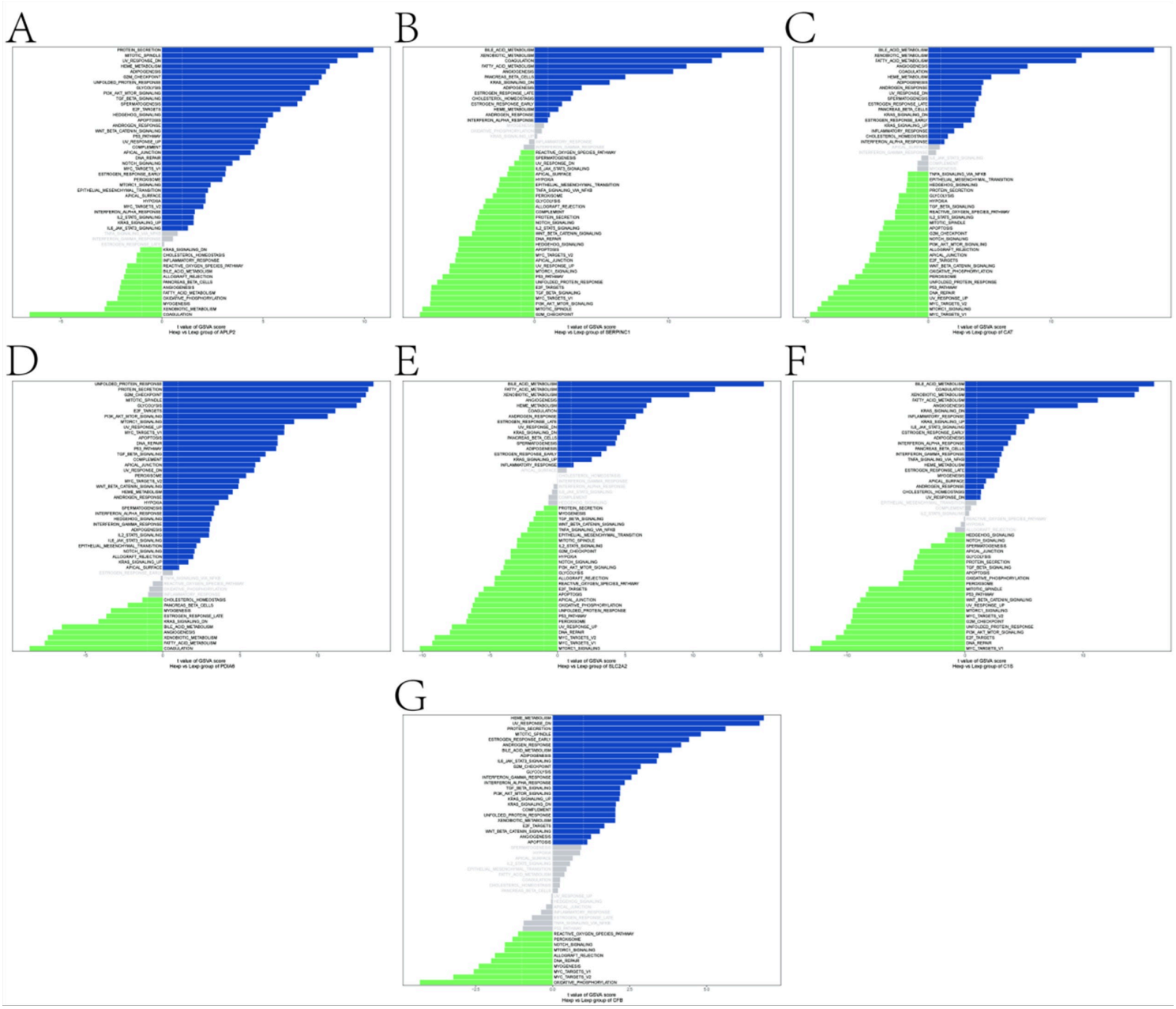


Figure 8

Stratification of prognostic marker expression reveals systemic regulation of functional pathways in hepatocellular carcinoma. (A-G) GSVA enrichment analysis of Hallmark pathways based on high/low expression groups of the markers.

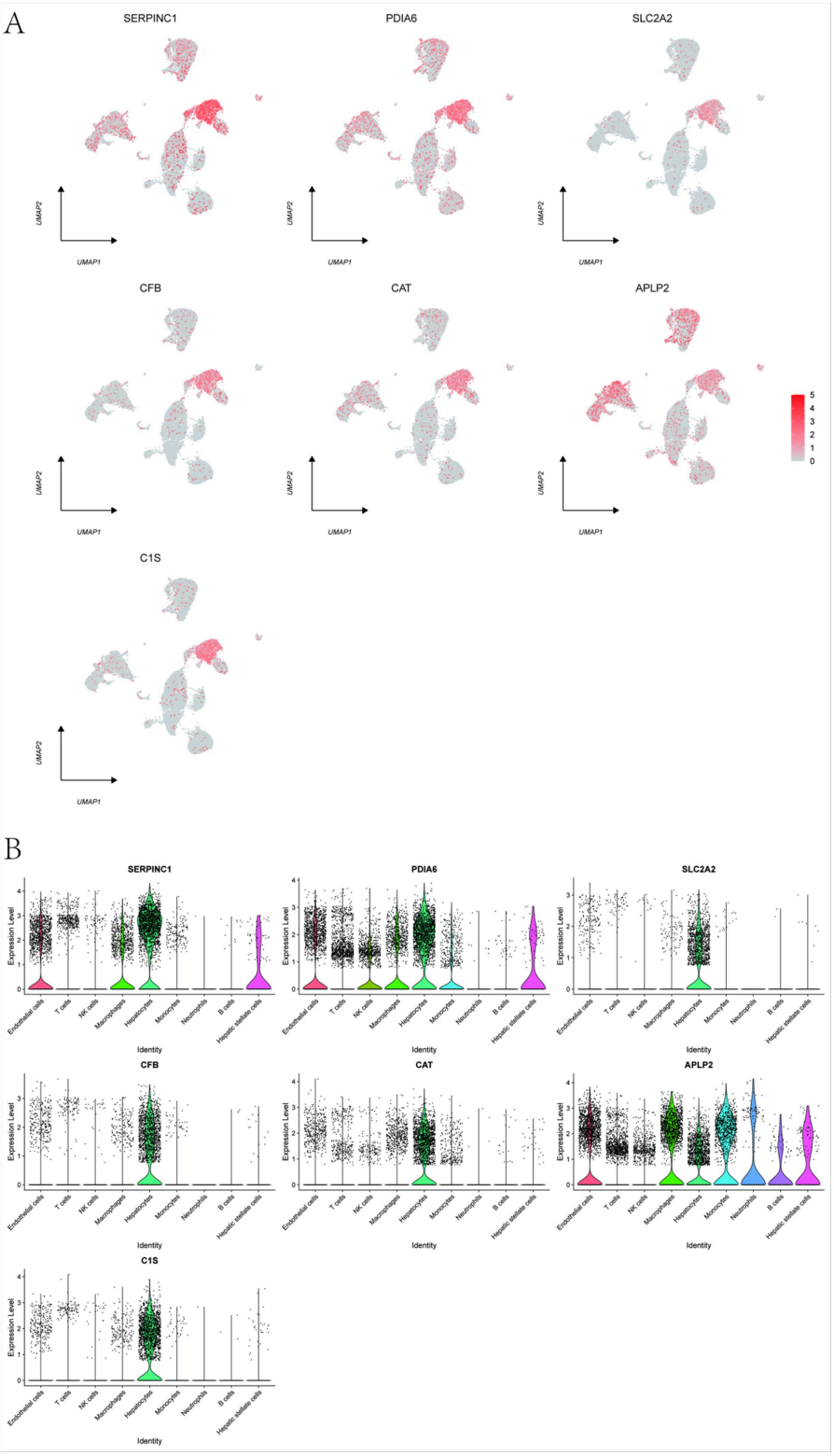


Figure 9

Single-cell spatial expression profiles of prognostic markers in the hepatocellular carcinoma microenvironment. (A) Expression distribution of the seven markers in UMAP space; (B) Cell type-specific expression quantification

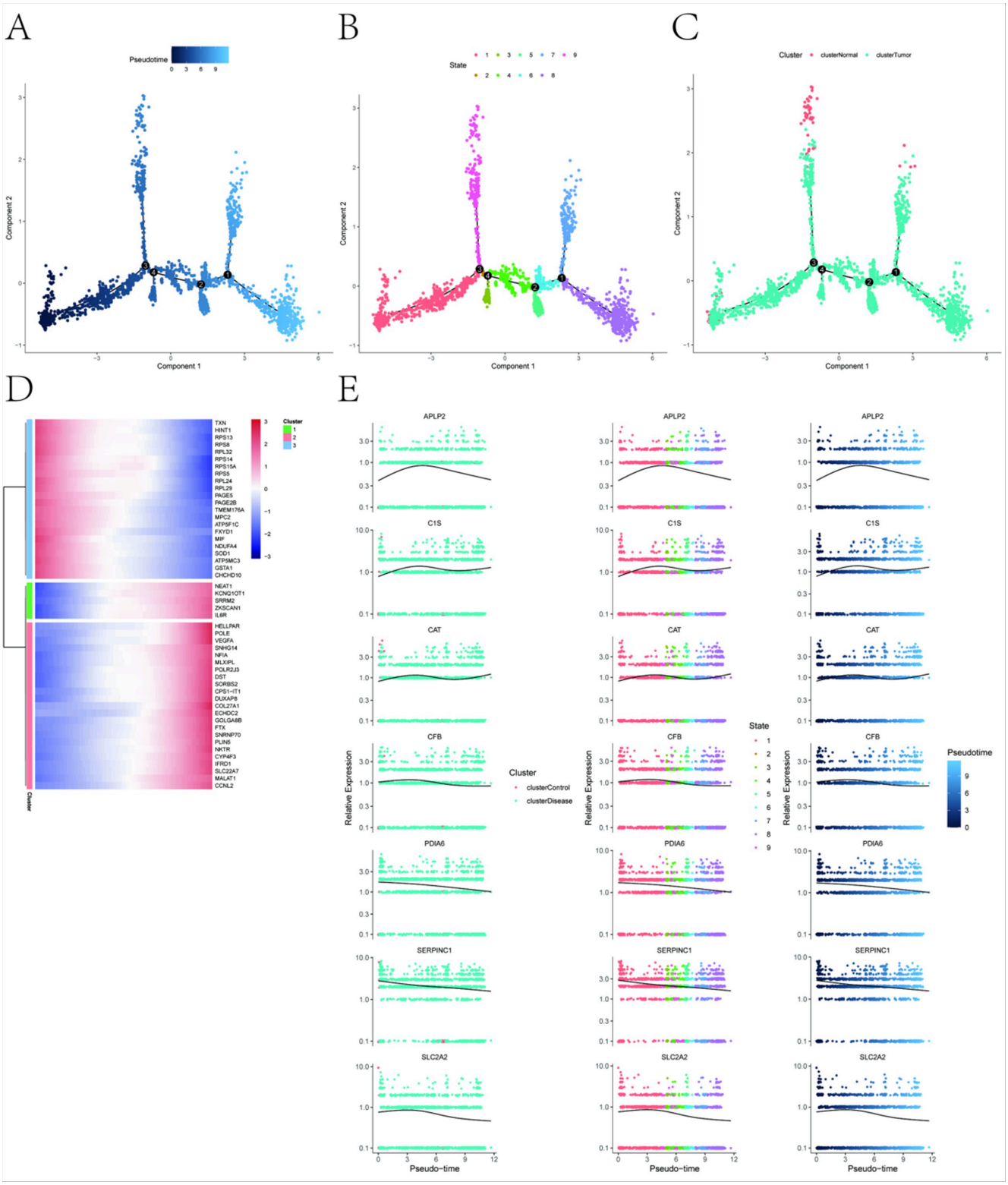


Figure 10

Integrated multi-omics dimensionality reduction analysis of hepatocellular carcinoma identifies core molecular driver modules. Principal component analysis (PCA)-based visualization of molecular networks: the top 50 principal components (accounting for >85% of explained variance) illustrate the distribution of key molecular modules, with Component 18 (complement pathway), Component 32

(glycolysis), and Component 155 (epithelial-mesenchymal transition [EMT]) identified as tumor-specific driver modules.

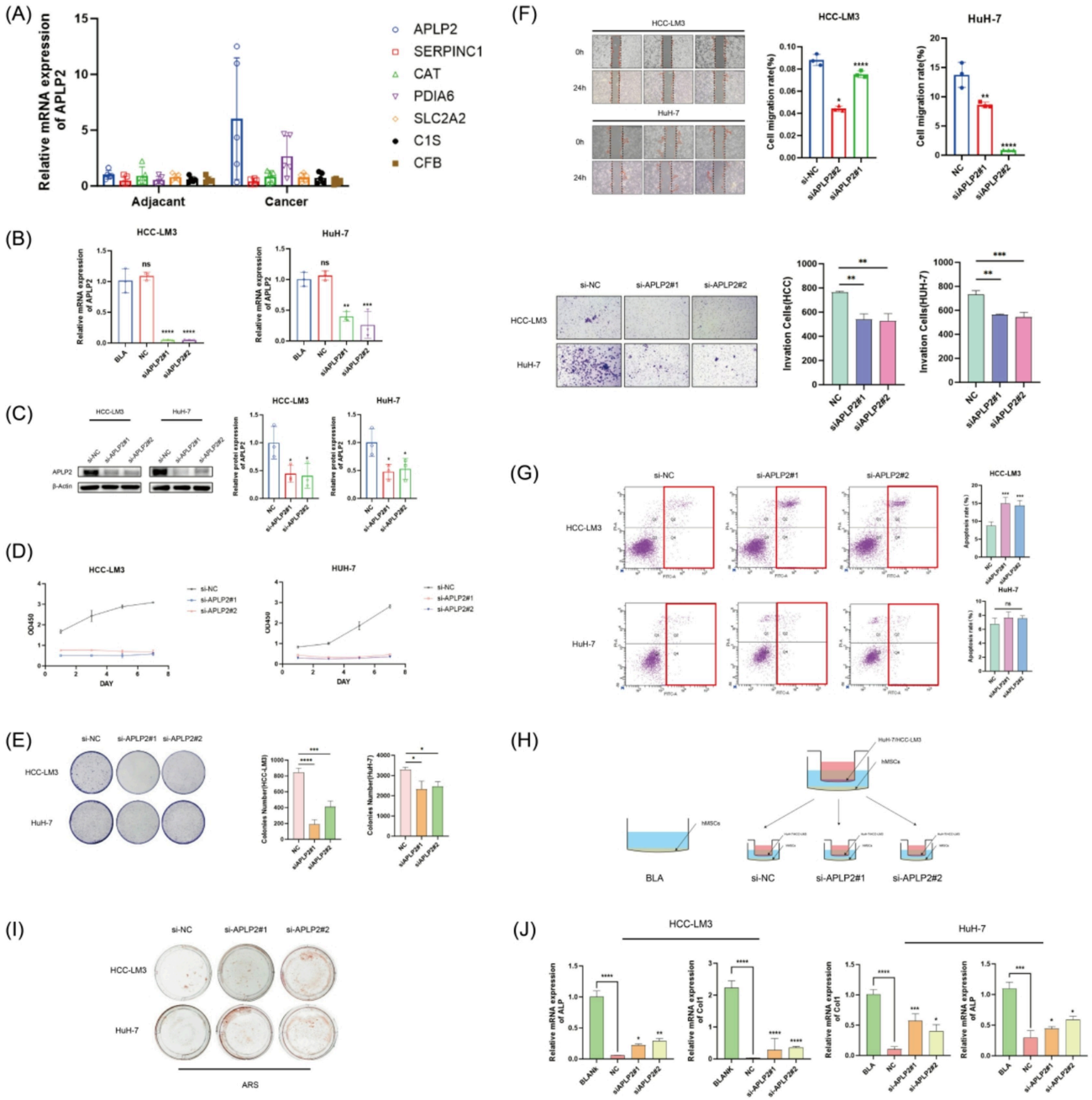


Figure 11

Cellular validation of functional changes following APLP2 knockdown. (A) Expression of seven key genes—*APLP2*, *SERPINC1*, *CAT*, *PDIA6*, *SLC2A2*, *C1S*, and *CFB*—in paracancerous and cancerous tissues from clinical patients; (B-C) qPCR and Western blot analyses to validate APLP2 knockdown efficiency; (D-

E) CCK8 assay and colony formation assays to assess cell proliferation; (F) Cell migration and invasion assays; (G) Flow cytometry to evaluate cell apoptosis; (H) Schematic representation of tumor cell–osteoblast co-culture; (I) Alizarin red staining assay; (J) PCR analysis to detect expression of osteogenesis-related markers *COL 1* and *ALP*.

Supplementary Files

This is a list of supplementary files associated with this preprint. Click to download.

- supplement.docx
- Fig.S1.tiff
- Fig.S10.tif
- Fig.S2.tiff
- Fig.S3.tiff
- Fig.S4.tiff
- Fig.S5.tiff
- Fig.S6.tiff
- Fig.S7.tiff
- Fig.S8.tiff
- Fig.S9.tiff